



## City Research Online

### City, University of London Institutional Repository

---

**Citation:** Camara, A., Nguyen, K., Ruiz-Teran, A. M. & Stafford, P. J. (2014). Serviceability limit state of vibrations in under-deck cable-stayed bridges accounting for vehicle-structure interaction. *Engineering Structures*, 61, pp. 61-72. doi: 10.1016/j.engstruct.2013.12.030

This is the accepted version of the paper.

This version of the publication may differ from the final published version.

---

**Permanent repository link:** <https://openaccess.city.ac.uk/id/eprint/12609/>

**Link to published version:** <https://doi.org/10.1016/j.engstruct.2013.12.030>

**Copyright:** City Research Online aims to make research outputs of City, University of London available to a wider audience. Copyright and Moral Rights remain with the author(s) and/or copyright holders. URLs from City Research Online may be freely distributed and linked to.

**Reuse:** Copies of full items can be used for personal research or study, educational, or not-for-profit purposes without prior permission or charge. Provided that the authors, title and full bibliographic details are credited, a hyperlink and/or URL is given for the original metadata page and the content is not changed in any way.

---

---

---

City Research Online:

<http://openaccess.city.ac.uk/>

[publications@city.ac.uk](mailto:publications@city.ac.uk)

---

# Serviceability limit state of vibrations in under-deck cable-stayed bridges accounting for vehicle-structure interaction

A. Camara<sup>1</sup>, K. Nguyen<sup>2</sup>, A.M. Ruiz-Teran<sup>1,\*</sup>, P.J. Stafford<sup>1</sup>

(1) *Department of Civil and Environmental Engineering, Imperial College London, South Kensington Campus, Exhibition Rd, London SW7 2AZ, United Kingdom*

(2) *Department of Mechanics and Structures, School Of Civil Engineering, Technical University of Madrid (UPM), Prof. Aranguren s/n, Madrid, Spain*

(\*) *Corresponding author*

---

## Abstract

Verification of the serviceability limit state of vibrations due to traffic live loads can be neglected in conventional types of concrete road bridges but becomes critical in the design of slender structures like Under-Deck Cable-Stayed bridges. The novelty of the work presented in this article is that an innovative vehicle-bridge interaction model is employed, in which realistic wheel dimensions of heavy trucks, road roughness profiles and the cross slope of the road are considered in nonlinear dynamic analyses of detailed three-dimensional finite element models. An extensive parametric study is conducted to explore the influence of the bridge parameters such as the longitudinal and transverse cable arrangement and the support conditions, in addition to the load modelling, road quality, the wheel size, the transverse road slope and the vehicle position and speed on the response of under-deck cable-stayed bridges. It has been observed that the vibrations perceived by pedestrians can be effectively reduced by concentrating the cable-system below the deck at the bridge centreline. The Fourier amplitude spectrum of the acceleration at critical positions along the deck proved that the response of Under-Deck Cable-Stayed bridges is not dominated only by contributions at

---

*Email addresses:* [Alfredo.camara@city.ac.uk](mailto:Alfredo.camara@city.ac.uk) (A. Camara<sup>1</sup>),  
[khanh@mecanica.upm.es](mailto:khanh@mecanica.upm.es) (K. Nguyen<sup>2</sup>), [a.ruiz-teran@imperial.ac.uk](mailto:a.ruiz-teran@imperial.ac.uk) (A.M. Ruiz-Teran<sup>1,\*</sup>), [p.stafford@imperial.ac.uk](mailto:p.stafford@imperial.ac.uk) (P.J. Stafford<sup>1</sup>)

Cite as:

A. Camara, K. Nguyen, A.M. Ruiz-Teran, P.J. Stafford (2014) Serviceability limit state of vibrations in under-deck cable-stayed bridges accounting for vehicle-structure interaction, *Engineering Structures*, 61: 61-72

the fundamental mode and, consequently, the conventional deflection-based methods are not valid to assess the users comfort. Instead, Vehicle-Bridge Interaction analyses are recommended for detailed design, considering the wheel dimensions if the pavement quality is bad and/or if the wheel radius is large. Finally, we verify through multiple approaches that the comfort of pedestrian users is more critical than that of vehicle users. However, the comfort of vehicle users is shown to be significantly affected when the road quality is poor.

*Keywords:*

vehicle-bridge interaction model; Under-deck cable-stayed bridges; moving vehicles; comfort; road roughness; disk model; vibration; serviceability; road traffic loading

---

## 1. Introduction

Verification of the Serviceability Limit State (SLS) of vibrations due to traffic live loads has historically been ignored in the design of conventional road bridges with reinforced and prestressed concrete decks. While this design approach is generally justified for traditional bridges, this does not imply that the approach can simply be translated to other less-conventional and slender concrete bridges, such as Under-Deck Cable-Stayed Bridges (UD-CSBs) [1]. UD-CSBs have been shown to be very efficient when used for medium spans under persistent [2, 3, 4, 5] and accidental situations such as sudden breakage of cables [6] or earthquake actions [7]. The very high efficiency of the cable stay system (with the stay cables working in tension and the struts and the deck working in compression) allows for more slender designs (depth-span ratio of 1/80 for medium spans of around 80 m) in comparison with conventional schemes. Internationally renowned structural engineers like Leonhardt, Schlaich, Virlogeux, Cremer and Manterola have designed remarkable bridges with this typology. Previous research on these bridges has also been recognised through the 2009 FIB diploma for research [8], which further demonstrates that there is active interest in these bridge types within the structural engineering community. Due to the large slenderness of the deck, these bridges are subjected to significant traffic-induced vibrations that cannot be neglected in the design. In fact, the depth of the deck is limited by the SLS of vibrations due to traffic load.

In order to develop design criteria for the SLS of vibrations due to traffic

live load, all of the components of the problem must be considered: the vibration source (movable vehicle or load), the vibration path (the structure), and the receiver (pedestrians or vehicle users). In short and medium span road bridges the most important source of vibration is the road traffic. In most cases pedestrians are the first users to feel discomfort. People inside vehicles are more tolerant to vibrations and are also partially isolated from these as a result of vibration mitigation measures incorporated into the vehicle [9]. Pedestrians are typically considered as the receiver of the vibration in codes, standards and research works, with the vehicle users' comfort being ignored as pedestrian comfort is usually only considered in footbridges. There are road bridges, mainly highway bridges, where the only users that should be considered for persistent situations are those inside the vehicles. The vibration felt by drivers and passengers is mainly transmitted through the floor of the cab as well as the seats and the highest ride vibrations occur in the vertical and fore-and-aft directions [10]. The maximum human sensitivity to vertical acceleration falls in the frequency range from 4 Hz to 12.5 Hz [11], higher than the first UD-CSBs and vehicle frequencies.

In practice, two types of analysis procedure are typically adopted in order to verify the SLS of vibrations due to traffic live load [1]: deflection- and acceleration-based methods. In the deflection-based methods the accelerations of the bridge under the frequent traffic live load are intended to be indirectly controlled by limiting the deflection due to a static load. Several codes and guidelines [12] indicate that under the live load the bridge deflection must be smaller than a limit of around  $L/1000$  (with  $L$  being the main span of the bridge) that has been prescribed on the basis of previous experience. This deflection limit dates back to the early 1930's and it is not sufficiently well justified for use in modern bridge design [13]. Another deflection-based method employed in codes [14] is a pseudo-static approach based on Smith's studies [9] in which the maximum vertical acceleration in the bridge is assumed to be directly proportional to the dynamic deflection at mid-span, by assuming that the response is governed by a single mode of vibration. Deflection-based methods are the traditional and most common approaches used by practicing engineers but their shortcomings are widely recognized and come from the assumption that the structure is dominated by the fundamental vibration mode. As will be confirmed in this paper, this is not appropriate for UD-CSBs.

The acceleration-based strategy is more rational since the recorded acceleration is directly compared to a selected comfort criterion that takes into

account the human perception of the vibration, which is particularly sensitive to vertical accelerations [15]. Several direct and indirect factors influence a pedestrian’s perception of vibration when crossing a bridge: the position of the human body (walking, standing or seated), exposure time, expectations regarding the likely vibration of the bridge based upon its visual appearance [16], height above ground, sound generated, user’s health [17] etc. Many studies have already established admissible vibration limits to meet different degrees of pedestrian comfort. This issue continues to receive attention from the academic community. A thorough state-of-the-art review for pedestrians was presented by [18].

The two main pedestrian comfort criteria used for bridge design (both for footbridges and road bridges with footpaths) are Irwin [17] and the British Standard [19]. Irwin [17] collected data about human response to vibration with respect to frequency and suggested maximum allowable limits for root-mean-square (r.m.s.) accelerations for bridges in the vertical direction. His work identified a frequency range of between 1 and 2 Hz, close to the typical natural frequency of UD-CSBs [4, 7]. Irwin’s recommendation distinguishes everyday use from storm conditions for which the admissible accelerations are multiplied by the factor of 6. On the other hand, the British Standard BS 5400: Part 2 [19] was the first design code to deal with vibration serviceability in footbridges and limits the peak vertical acceleration (rather than r.m.s.) to  $a_{\text{lim}} = 0.5\sqrt{f}$  (where  $f$  is the fundamental frequency of the structure in Hz, and  $a_{\text{lim}}$  is in units of  $\text{m/s}^2$ ). The main contributions in relation to the comfort of vehicle users have been provided by Griffin [20].

In relation to the description of the vibration source, which is essential in the acceleration-based approach, two main methods are employed to describe the traffic loading. The simplest solution is to ignore the dynamic characteristics of the vehicle (mass, damping and stiffness) and to define time-varying point loads applied to the deck nodes along the path that will be followed by the vehicle. In this case, triangular functions are employed to describe the load amplitude applied at each node against time, see Figure 1(a). However, this Point Load (PL) model is not able to capture the Vehicle-Bridge Interaction (VBI) and the influence of the pavement conditions, which have an important impact upon the overall system dynamics [21, 22] and particularly influences the vibrations perceived by users. Moreover, if the bridge does not have footpaths the Point Load model ignores the vibration sensed by the only users of the structure, i.e. people within the vehicles. Current research on VBI typically employs a Multi-Degree-Of-Freedom (MDOF) model of the

vehicle to describe the flexibility and damping of the tyre and suspension systems, allowing for the yaw, roll and pitching motions of the truck body to be captured. The H20-44 truck model defined by the American Association of State Highway and Transportation Officials (AASHTO) specifications [12] is appropriate for the SLS of vibrations since it may combine both heavy vehicle weight (18.6 t) and high velocities (up to 120 km/h). This model has been employed by several authors [21, 23] and has 7 degrees of freedom which are described graphically in Figure 1(b). An important advantage of the vehicle model interacting with the bridge (VBI) is the ability to represent the pavement roughness. According to [21, 22], among many other authors, the road surface roughness may be defined by means of an ergodic zero-mean stationary Gaussian random profile of imposed displacements ( $r(x)$  in Figure 1(b)) at the nodes of the vehicle in contact with the bridge.

In the present article the dynamic response of UD-CSBs is studied, focusing on the comfort of pedestrians walking along the sidewalks but also considering the vibrations perceived by people inside the vehicle. The paper starts by presenting the canonical UD-CSBs studied, the vehicle model and the contributions of the governing vibration modes. The results of an extensive number of nonlinear dynamic analyses are discussed next, clearly distinguishing the features related to the vehicle action (e.g. the wheel radius) from the influence of the structural configuration. The comparison between the results obtained with current simplified design approaches completes this work. These models are used to identify the most suitable bridge configurations to enhance the bridge behaviour under live load. In addition, a set of design criteria is ultimately proposed.

## 2. Definition of the studied bridges and vehicle

This paper is focused on medium span (80 m) under-deck cable-stayed bridges with in-situ prestressed concrete decks. A set of bridges designed by Ruiz-Teran and Aparicio [4] will be used for this study. Figure 2(a) presents the elevation of the studied bridges with two or multiple (15) diverting struts. Figure 2(b) presents the two considered transverse cable arrangements, designed with a concentrated or expanded layout. These configurations are selected so as to cover the current trends in design.

The deck has been designed to support two road lanes (3.5 m wide each). Two heavy vehicles of 400 kN crossing the bridge at 60 km/h described as

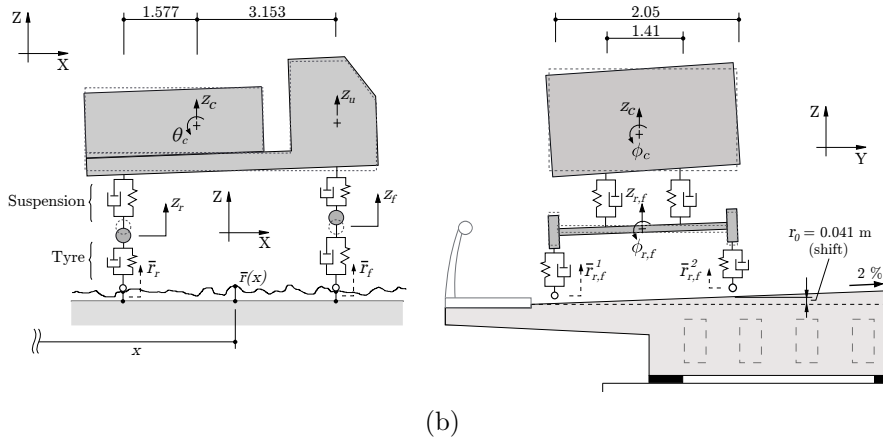
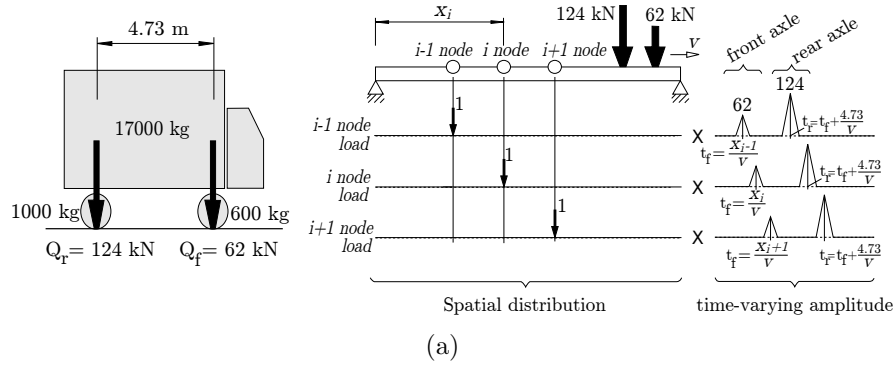


Figure 1: Vehicle model in dynamic analysis; (a) H20-44 truck equivalent wheel loads ( $Q$ ) and time-dependent amplitude in the Point Load (PL) model; (b) MDOF model of the H20-44 truck in the model with Vehicle-Bridge Interaction (VBI), the 7 DOF are the vertical displacement of body, front and rear axle ( $z_c, z_f, z_r$ ), the pitch displacement of the body ( $\theta_c$ ), the roll displacement of the body ( $\phi_c$ ) and the front and rear axle rolling ( $\phi_f, \phi_r$ ).  $\bar{r}(x)$  is the roughness profile filtered according to the disk model defined in section 4.1.  $z_u$  is the vertical displacement of the driver cabin. Units in metres.



point loads and using the British Standard criteria [19] were employed in the design of the bridges [4].

The maximum vehicle eccentricity in this original design case is limited to  $e = 2.475$  m as shown in Figure 2(b). In this work the lane distribution is modified from the original design in order to accommodate vehicles with larger eccentricities that directly effect the flanges. Figure 3(a) presents the new configuration with three road lanes and narrower sidewalks. Three load cases have been studied: (i) Load Case I with a centered passing vehicle ( $e = 0$  m); (ii) Load Case II with an eccentric vehicle in the three-lane configuration ( $e = 3.57$  m); and (iii) Load Case III with an eccentric vehicle in the two-lane configuration ( $e = 2.475$  m), shown in Figure 2(b).

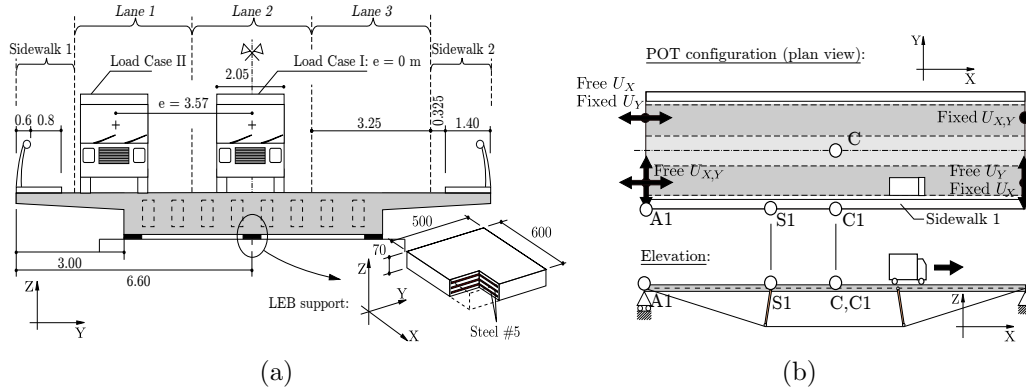


Figure 3: (a) cross-section of the bridge at the abutment and Load Cases (LC) considered in the 3-lane road distribution, including the Laminated Elastomeric Bearings (LEBs); (b) plan view and elevation of the bridge with the POT support configuration, besides labels at key deck positions employed to refer the ongoing results. Units of the deck in metres and units of the LEB in millimetres.

Two different types of supports have been considered:  $500 \times 600 \times 70$  mm Laminated Elastomeric Bearings (LEBs) and POT bearings. Figure 3(a) illustrates the location of LEBs at the abutment. Each LEB has been modeled by means of linear springs representing the vertical and horizontal stiffness, obtained through the expressions provided in [24]. On the other hand, the POT bearings are infinitely stiff in the vertical direction and completely restrain, or release, horizontal movements according to the ‘classical’ layout for simply supported bridges [25] depicted in Figure 3(b). In this figure several key points along the deck are highlighted and labeled to facilitate the discussion of the results in the following sections. Position A1 is located on the

sidewalk close to the eccentric vehicle (sidewalk 1 in Figure 3) over the support at the abutment where the vehicle enters onto the bridge (the ‘left’ end of the bridge as shown in Figure 3(b)); S1 is on sidewalk 1 at the strut-deck connection; C1 and C are located at mid-span, respectively on sidewalk 1 and the centreline (no eccentricity). Table 1 summarizes the proposed structures resulting from the combination of the aforementioned design choices, and the keywords employed hereafter.

Table 1: Summary of UD-CSB configurations.

Keyword	No. struts	Transverse arrangement	Bearings
BI-CONC-LEB	2	Concentrated	LEB
BI-CONC-POT	2	Concentrated	POT
BI-EXP-LEB	2	Expanded	LEB
MULT-EXP-LEB	15	Expanded	LEB

Rigorous finite element models have been developed to describe the dynamic behaviour of the proposed light-weight UD-CSBs, in which the proper mass distribution is a key factor. Shell elements with proper offsets of the element plane to avoid the mass superposition at the intersections of the webs and the slabs [26] have been adopted in the deck. The mesh density (approximately 1 m long elements) is defined in order to represent the local flange modes of the deck with sufficient accuracy. The total number of nodes in the bridge with two concentrated struts (BI-CONC-LEB) is 3387.

External platforms (30 m long beyond the bridge length) are connected to the upper slab at both abutments in order to stabilize the response of the vehicle before it enters onto the deck and after it leaves the bridge. The platforms are connected to the ground by vertical springs that simulate the pavement and soil flexibility. The joint connecting the platform with the upper slab of the deck allows for relative movements in all directions, representing a real bridge joint.

Standard elastic material properties have been taken from relevant Eurocodes. This study is focused on the Serviceability Limit State (SLS) of vibration and as a result, possible concrete damage or any other potential source of degradation of the materials does not need to be considered. The concrete always work in compression during the dynamic analysis due to the initial stress introduced by the active reinforcement. The elastic modulus of the concrete in the deck is 35 GPa. The steel representing passive reinforcement and diverting struts is B-500 SD and S355 respectively with an elastic

modulus of 210 GPa. The steel in the active tendons inside the deck and the cable-system below the deck has an elastic modulus of 190 GPa.

The internal and external tendon prestress, in addition to the self-weight of the structure and the vehicle, are applied in the first step of the analysis and the initial deformed configuration is statically obtained, prior to the entrance of the moving vehicle. In the second step of the analysis the dynamic response of the bridge and the vehicle is obtained. The loads that are transmitted by the tyres of the moving truck to the bridge surface are functions of the bridge deflection and the dynamic response of the vehicle. The vehicle-bridge interaction is defined by means of a node-to-surface contact resulting in a coupled system of equations with feedback between the vehicle and the bridge that requires the use of an iterative procedure. The HHT implicit integration algorithm [26] is adopted in this stage with a constant time step of 0.001 s. This time step is small enough to accurately capture high-frequency vibrations (above the limit of 45 Hz suggested by [21]) and to allow for the precise definition of the roughness profile. The dissipation mechanisms of the structure are represented in the dynamic analyses using Rayleigh damping, while additional energy is dissipated through the rigorous definition of the damping system associated with the vehicle. Following an initial sensitivity study, the influence of the structural damping was observed to be negligible (provided that reasonable values are considered). The same distribution of damping is considered in all cases, which is obtained by imposing a damping ratio of 2 % in both the fundamental mode (0.75 Hz, see Table 2) and that corresponding to the maximum frequency of interest: 45 Hz. This damping ratio of 2 % have been measured in the Glacis and Takehana bridges [27, 28] which are UD-CSBs.

The MDOF model of the H20-44 truck illustrated in Figure 1(b) is employed in this study to define the vehicle action, exploiting the capabilities of the Abaqus finite element software [26] for multibody dynamics. Table 3 presents the frequencies and modal damping associated with the first vibration modes of the vehicle. A detailed definition of the mechanical properties of the 7 DOF vehicle model was reported elsewhere [21]. The Vehicle-Bridge Interaction (VBI) scheme, which introduces two innovative features (disk model and cross slope, both to be defined later), is discussed in the following sections. In addition, in the last section of this paper a simplified dynamic analysis with moving loads representing the vehicle action is included for comparative purposes.

Table 2: First vertical and torsional vibration modes in the proposed structures.  $f$  is the frequency in Hz. The mode shape is included in Figure 4. ‘S’ and ‘A’ denote that the mode is Symmetric or Antisymmetric with respect to the mid-span section respectively.

Structure	Mode No.	$f$ [Hz]	Description
BI-CONC-LEB	3	0.78	1st vertical flexure (S)
	4	1.00	2nd vertical flexure (A)
	6	1.73	1st torsion
BI-CONC-POT	1	0.78	1st vertical flexure (S)
	2	1.00	2nd vertical flexure (A)
	3	1.73	1st torsion
BI-EXP-LEB	3	0.78	1st vertical flexure (S)
	4	0.99	2nd vertical flexure (A)
	6	1.70	1st torsion
MULT-EXP-LEB	3	0.75	1st vertical flexure (S)
	4	1.01	2nd vertical flexure (A)
	6	1.65	1st torsion

### 3. Modal study

A valuable understanding of the dynamic response of these structures under heavy vehicles can be anticipated by the simple inspection of the vibration modes. Table 2 describes the first vibration modes for the considered bridges and will help to explain the results presented in the following sections. In bridges with LEB supports, the horizontal rigid modes involving exclusively the deformation of these devices have associated frequencies of 0.70 and 0.73 Hz in transverse and longitudinal directions respectively. However, horizontal modes are not included in Table 2 because they hardly affect the vertical response of the bridge under passing vehicles. The small influence of the longitudinal and transverse cable-system arrangement in the first vertical flexural and torsional modes of the deck is observed in Table 2. These modes are also not appreciably influenced by the support typology due to the large stiffness of both LEB and POT devices in the vertical direction.

The study of the participation of vibration modes traditionally ignores the dynamic excitation and is focused on parameters obtained exclusively from the structure, like the participation factors or the modal mass. Nonetheless, the excitation cannot be ignored since depending on the vehicle eccentricity or velocity (among others) the contribution of different modes can be amplified or cancelled. Since the direct dynamic analysis employed is not based on

modal decomposition, the Discrete Fourier Transform (DFT) of the time-histories of acceleration is used here in order to distinguish the participation of different vibration modes (Figure 4). The pavement is assumed to be perfectly flat without irregularities (i.e. the road roughness is neglected) in this section to avoid effects that could mask the contribution of the bridge modes. From Figure 4 the following important remarks are extracted:

- (i) if the passing vehicle is eccentric with respect to the bridge axis (Load Case II and III in Figures 3(a) and 2(b)) the global torsional modes, with movement of the deck and the cable-system, are excited (e.g. the 6<sup>th</sup> mode,  $f = 1.73$  Hz, as shown in Figure 4(a)). However, vertical bending modes are excited in an identical manner regardless of the vehicle eccentricity (e.g. 3<sup>rd</sup>, 7<sup>th</sup> and 12<sup>th</sup> modes);
- (ii) an important group of vibration modes with frequencies ranging from 20 to 40 Hz and involving local vertical flexure of the flanges is activated when the vehicle wheels are located over the flange of the deck (Load Case II) as shown in Figure 4(a), these local flange modes contribute to the vertical acceleration along the sidewalk and consequently affect the comfort of pedestrians;
- (iii) the closer the position to the abutment (point A1 in Figure 3(b)), the larger the contribution of high-order modes to the vertical response (Figure 4(b)). From these results it is clear that the fundamental mode (first order vertical flexure of the deck) alone cannot describe the rich frequency content of the acceleration response of UD-CSBs under moving vehicles (this is especially true for the sidewalks). At the connection with the struts (point S1) the first antisymmetric mode (4<sup>th</sup> mode,  $f = 1.00$  Hz) becomes important (comparable to the contribution of the fundamental symmetric mode); and,
- (iv) in agreement with the study of Yang and Lin [29] in conventional simply-supported bridges, the first bridge frequencies are much more important than the driving frequency ( $f_v = v/2L = 0.2$  Hz if  $v = 120$  km/h) for the acceleration recorded at the deck in different positions. Analogous results have been obtained for different vehicle velocities and structural configurations.

The first three vehicle vibration modes are included in Table 3 and are in agreement with those reported by Marchesiello *et al.* [21]. From the response

Table 3: Vehicle modal parameters in the first three vibration modes.  $f$  is the frequency and  $\xi_v$  is the modal damping ratio.

Mode No.	Description	$f$ [Hz]	$\xi_v$ [%]
1	Body roll	0.92	34
2	Body pitch	0.93	52
3	Body pitch & heave (vertical motion)	1.14	29

of the vehicle in the time-domain it has been verified that resonant effects are not relevant. This is explained by the relatively short length of the bridge (80 m), which is not enough to allow more than 2 to 4 complete cycles of the first vehicle modes while it is crossing the bridge with the range of velocities considered (60 - 120 km/h), and the lack of repetitive loading (such as those acting in railway bridges).

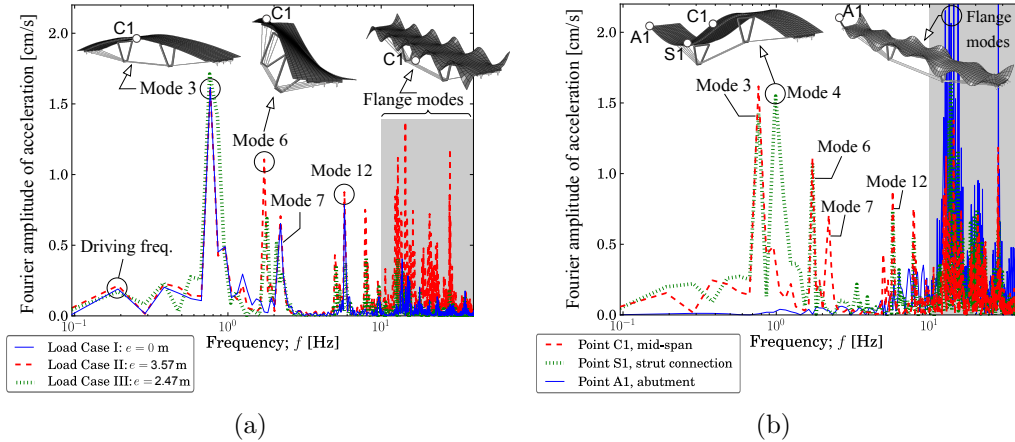


Figure 4: Frequency content of deck vertical acceleration when the H20-44 truck (VBI model) crosses the deck with  $v = 120$  km/h and no irregularity (perfect road); (a) effect of the vehicle eccentricity ( $e$ ) at point C1 (included in Figure 3(b)); (b) effect of the position along sidewalk 1 where the response is measured (Load Case II). The shape of important vibration modes of the structure is included. BI-CONC-LEB bridge.

#### 4. Effect of vehicle-related aspects on the dynamic response of under-deck cable-stayed bridges

An extensive number of analyses with different parameters related to the vehicle action is discussed in this section. Two innovative features are introduced in the VBI model that were routinely ignored in previous works: the finite dimensions of the vehicle wheels and the transverse slope of the pavement.

##### 4.1. Disk model for roughness definition

The roughness profile,  $r(x)$ , is an imposed displacement that is generated using the following spectral-density based function [22]:

$$r(x) = \sum_{k=1}^N \sqrt{2\varphi(n_k)\Delta n} \cos(2\pi n_k x + \theta_k) \quad (1)$$

in which  $x$  is the position of the point where the profile is defined with respect to the left end of the external platform (Figure 1(b));  $n_k$  is the spatial frequency [cycle/m],  $n_1$  and  $n_N$  are respectively the lower and upper cut-off frequencies;  $\Delta n$  is the increment between successive frequencies;  $\theta_k$  is a random phase angle uniformly distributed from 0 to  $2\pi$ ; and  $\varphi(n_k)$  is the Power Spectral Density (PSD) function [ $\text{m}^3/\text{cycle}$ ] for the road surface elevation. In the present study, the following PSD function defined by ISO 8608:1995 [30] is employed:

$$\varphi(n_k) = a \left( \frac{n_k}{0.1} \right)^{-2} \quad (2)$$

where  $a$  is the spectral roughness coefficient [ $\text{m}^3/\text{cycle}$ ] whose value is chosen depending on the road condition. According to ISO 8608:1995 the following road qualities and keywords to refer the results are considered in this work: very good (road A)  $a = 16 \times 10^{-6}$ ; good (road B)  $a = 64 \times 10^{-6}$ , regular (road C)  $a = 256 \times 10^{-6}$ , bad (road D)  $a = 1024 \times 10^{-6}$ .

Although the MDOF vehicle model defines the wheels as dimensionless points where the road profile is imposed (see Figure 1(b)), it is clear that the finite wheel dimensions prevent the tyre-pavement contact from following the entire profile. Depending on the wheel radius and the road roughness there may be ‘deep valleys’ in which the lower part of the wheel does not contact the profile generated by expression (1), as shown in Figure 5. To complete the picture, the contact occurs through a finite footprint area rather than

at a single point. These complex effects are traditionally summarized by limiting the upper cut-off frequency to  $n_N = 10$  cycle/m when generating the roughness profile [21, 31, 32], as an approximate way to take into account that high frequencies in the roughness profile are filtered by the aforementioned effects. More rigorously, Captain [33] proposed a disk model with a rigid tread band that yields results similar to models with finite footprints, and is also generally conservative. In this approach the filtered profile ( $\bar{r}(x)$ ) is obtained from the original one ( $r(x)$ ) as the locus of the wheel centre in Figure 5, and is directly imposed to the vehicle model. The position of the contact point between the original profile and the wheel (point P) is obtained following the procedure suggested by Chang *et al.* [34] and illustrated in Figure 5. Once the contact point is located, the filtered profile is defined as follows:

$$\bar{r}(x) = r(x_P) + \sqrt{R^2 - d^2} + r_0 \quad (3)$$

where  $r(x_P)$  is the distance between the reference surface and the original road irregularity at the contact point (P) obtained with equation (1);  $d = x_P - x_o$  and  $R$  is the wheel radius. Figure 5 describes these variables. The parameter  $r_0$  is introduced in this work to consider a 2 % cross slope of the road, it is a constant shift added only to the wheels which are closer to the bridge centreline ( $\bar{r}_{r,f}^2$  in Figure 1(b)):  $r_0 = 0$  in Load Case I and  $r_0 = 4.1$  cm in Load Case II and III. The procedure is repeated at each point of the original profile to obtain the filtered roughness in the complete road length (including the bridge deck and the external platforms).

Although the disk model realistically filters out the high profile frequencies, the ‘traditional’ cut-off frequencies  $n_1 = 0.01$  and  $n_N = 10$  cycle/m are maintained because the measured data of real road irregularities reported by [30] are below 10 cycle/m. The disk model is implemented for each of the four wheels of the H20-44 MDOF truck. The spatial correlation between the roughness in transverse direction is assumed negligible and, consequently, independent profiles are generated for the wheels on the vehicle sides 1 and 2; this is respectively represented by the imposed displacements  $\bar{r}_{r,f}^1$  and  $\bar{r}_{r,f}^2$  at the wheels in Figure 1(b). In agreement with [35], a set of ten profiles is generated by modifying the random phase angle  $\theta_k$  in equation (1), one per each side of the car, in order to obtain meaningful results from a statistical point of view. The average (represented by the symbol  $\mu$ ) of the results obtained by applying each roughness profile is reported hereafter, in addition

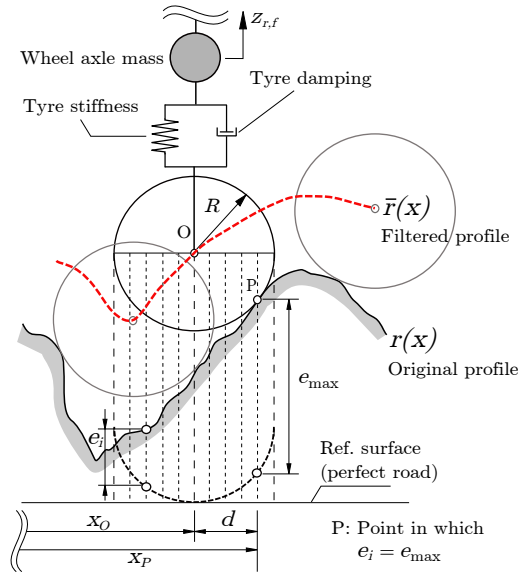


Figure 5: Disk model and subdivision of the wheel to obtain the contact point in each point of the road profile.  $z_r$  and  $z_f$  are the vertical DOFs of the wheel axles defined in the MDOF vehicle model in Figure 1(b). The roughness is intentionally exaggerated in vertical direction to improve the visibility of the model.

to the standard deviation ( $\sigma$ ) to provide information on the dispersion obtained with respect to the average. To further improve the understanding of the precision of the response estimates presented in this work, the 95% confidence interval in the estimate of the mean response can be obtained by compressing these standard deviation ranges to be 71.5% of what is shown in the figures hereafter (this value reflects the Student t statistic corresponding to the 95% confidence interval as well as the standard error for our particular sample size).

In order to illustrate the influence of the road irregularity filtered by different tyre models on the vertical response of the bridge, Figure 6(a) presents the average ( $\mu$ ) peak vertical acceleration along the deck centreline when the vehicle crosses the bridge with a velocity of 60 km/h and is completely centered (Load Case I), considering different wheel radii and a road pavement with regular quality (road C) as well as a ‘perfect’ road without irregularities. The dispersion of the results within the set of ten profiles is represented as a coloured band centered on the average value, the band width corresponds to the mean plus and minus one standard deviation at each point ( $\pm\sigma$ ). In

order to not excessively clutter the figure, this band is included only for one case, but similar deviations have been obtained in other cases. As expected, the disk model yields lower accelerations in comparison with the conventional point model (where  $r(x)$  is directly applied to the wheels) since the high-frequency content of the imposed roughness is unrealistically high in the latter case, even considering the traditional upper cut-off frequency of  $n_N = 10$  cycles/m in the profile generation. The difference between tyre models is higher as the road quality worsens and the wheel radius increases. If the road is a typical well-maintained highway (road A) and the wheel radius of the truck is standard (i.e.  $R = 0.3$  m) the point load and the disk models give similar results because the wheel dimension is much larger than the roughness ( $R \gg r(x)$ ) and the contact point is nearly aligned with the vertical line crossing the wheel center ( $r(x) \approx \bar{r}(x)$  in expression (3)). In these cases the conventional model and the disk model lead to results that are not statistically different, taking into account their dispersion. However, in regular-quality roads (type C) the peak acceleration considering the 30 cm radius wheels (conventional in 18 t trucks) is reduced by more than 40 % in comparison with the point contact (Figure 6(a)). If the road quality is not very good and/or if the vehicle wheel has a radius above 30 cm, the disk model should be employed to obtain accurate results in the bridge and the vehicle responses, in agreement with Chang *et al.* [34]. The results presented hereafter adopt the disk model with a wheel radius of 30 cm.

In agreement with [22], Figure 6(a) also highlights the importance of the road maintenance on the bridge response and, consequently, on the pedestrian's comfort. If the road quality is regular (road C), which can represent the status of 'minor' or 'secondary' roads, the maximum vertical acceleration recorded is up to 7 times higher than the situation with a perfect pavement (no irregularity), and the maximum acceleration allowed by BS 5400 [19] is clearly exceeded.

#### 4.2. Cross slope of the road

Due to the cross slope of the road, the wheel closer to the central axis of the deck is higher than the outer wheel (if the vehicle is eccentric), as represented in Figure 1(b). In this study a shift equal to  $r_0 = 4.1$  cm in equation (3) is imposed to the filtered road profile at the wheels closer to the centreline ( $\bar{r}_{r,f}^2$  in Figure 1(b)) if the vehicle is eccentric (Load Case II or III). The cross slope of the road has not been considered before in studies on road bridges subjected to moving vehicles. Figure 6(b) includes

the peak vertical acceleration along sidewalk 1 when the cross slope of the road is included or ignored (road type C). The average peak acceleration obtained when considering the cross slope is typically above that resulting when it is ignored, in some parts of the bridge the difference is up to 20 %. However, taking into account that the standard deviation is around 30 % in the same sections, the difference between the averaged responses in both cases is mainly explained by the variability of the results with independent road profiles. It could be concluded that the influence of the cross slope on bridge accelerations is weak. For completeness, the shift representing the cross slope is applied hereafter if the vehicle is eccentric.

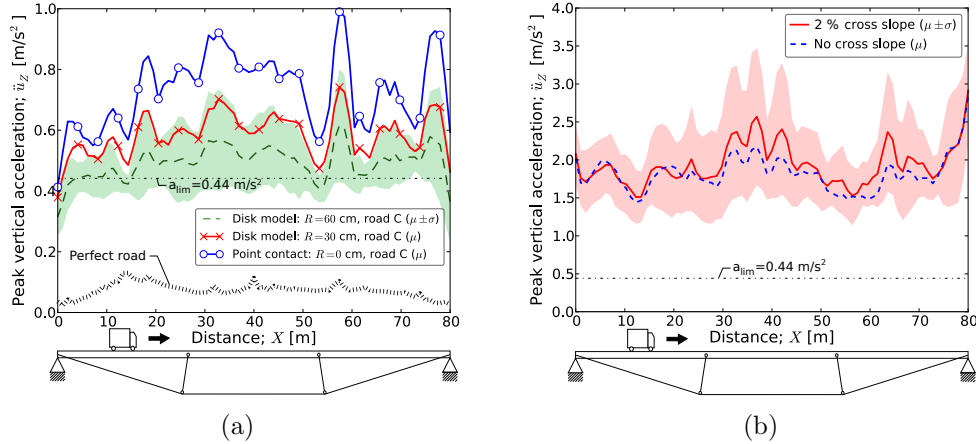


Figure 6: Influence of the specific features introduced in the VBI model on the peak vertical acceleration; (a) effect of the wheel radius in disk model VS the conventional point contact, results recorded along the deck centreline,  $v = 60$  km/h, Load Case I; (b) effect of the cross slope of the pavement in the response along sidewalk 1,  $v = 120$  km/h, Load Case II, regular pavement (road C). BI-CONC-LEB bridge. The maximum peak acceleration allowed by BS 5400 ( $a_{lim}$ ) is included as a reference.

#### 4.3. Influence of vehicle eccentricity

From the frequency domain analysis in Figure 4(a) an initial appreciation for the strong influence of the vehicle position across the deck width was obtained. Figure 7(a) presents the peak vertical acceleration obtained along the whole of sidewalk 1 when the vehicle velocity is  $v = 100$  km/h and the pavement is very good (road A). This figure again illustrates the significant difference between accelerations that are induced between a vehicle travelling

along the centre of the bridge, or with eccentricity. In this case, if the vehicle is eccentric (Load Case II or III) the admissible acceleration established by BS 5400 [19] is clearly exceeded along the whole sidewalk, even for high-quality roads. However, when the same vehicle crosses the bridge down its centreline the criterion is satisfied (Load Case I).

Two classes of vibration modes, activated if the vehicle action is eccentric, explain the increment of the vibration: (i) global torsional modes involving the rotation of the deck and the cable system along the longitudinal axis ( $X$ ), e.g. the 6<sup>th</sup> mode in bridges with LEB supports ( $\approx 1.7$  Hz); and (ii) local modes involving vertical deformation of the flange that are mainly excited if the vehicle is located over the lateral cantilevers, having frequencies in the range of 20 to 40 Hz. The frequencies and mode shapes associated with some of these modes are shown in Figure 4(a). The difference between both effects is clear in Figure 7(b), where the peak accelerations across the deck width are collated regardless of the longitudinal position in the deck where they are measured. The global torsion activated with the eccentric vehicle increases the vertical response of the bridge in both sidewalks, whilst local flange modes further increase the vertical acceleration in the sidewalk closest to the vehicle (sidewalk 1). Local flange modes are triggered mainly in Load Case II because the vehicle is located over the flange. However, the vibration resulting in this case is similar to that obtained when the eccentric vehicle does not affect the flange (Load Case III) and suggests that global torsion is more important than local flange flexure.

The assessment of the SLS for vibrations in sidewalks is especially important because pedestrians are very sensitive to vibrations. Considering BS 5400, the acceleration limit would be exceeded in both sidewalks if the vehicle is eccentric. This result has been observed for every road quality and vehicle velocity between 60 and 120 km/h. If the vehicle is completely centered (Load Case I), the distribution of peak vertical accelerations in the deck width is almost uniform because the response is governed by the vertical flexure modes.

#### *4.4. Influence of vehicle velocity*

A reasonable range of vehicle velocities ranging from 60 to 120 km/h, in increments of 10 km/h, has been considered. Below 60 km/h the dynamic effects associated with the truck are small. On the other hand, 18 t trucks are not expected to exceed velocities of 120 km/h. The peak vertical acceleration in the deck along sidewalk 1 for different vehicle velocities is presented

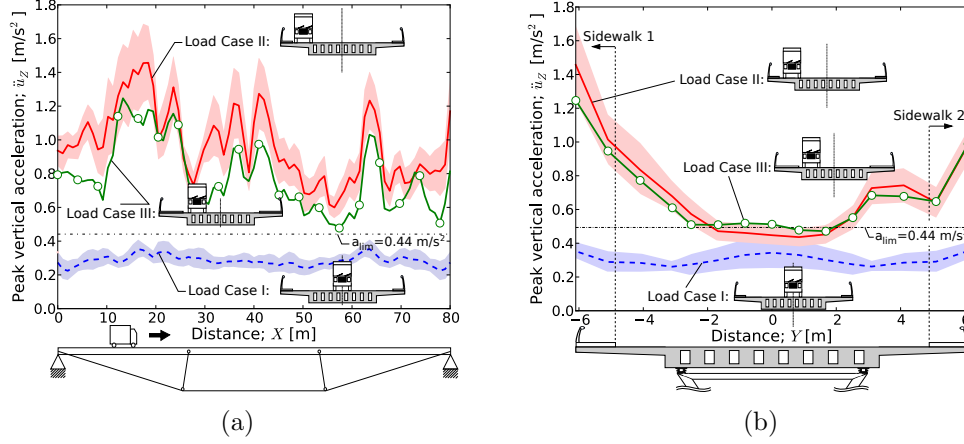


Figure 7: Influence of vehicle eccentricity; (a) peak vertical acceleration along sidewalk 1 (the one close to the vehicle); (b) peak vertical acceleration in the whole bridge for different positions across the deck width. BI-CONC-LEB bridge with very good pavement (road A). Vehicle velocity:  $v = 100 \text{ km/h}$ . The maximum acceleration allowed by BS 5400 ( $a_{\text{lim}}$ ) is included as a reference.

in Figure 8. The driving frequency  $f_v = v/2L$  ranges from 0.1 Hz to 0.2 Hz in the interval of velocities studied, which are far away from any bridge vibration mode. This explains why, if the road is perfect, the peak acceleration of the deck always increases with the vehicle velocity. However, even if small pavement irregularities are introduced (road A) additional bridge and vehicle frequencies are excited and these act to exacerbate the responses for particular vehicle velocities, e.g.  $v = 80 \text{ km/h}$  in Figure 8. No clear trend allows for the identification of these velocities since they depend on the road quality and vehicle eccentricity. In the majority of studied cases,  $v = 120 \text{ km/h}$  is the most unfavorable velocity (in the range of reasonable velocities for the heavy vehicle considered in this study).

## 5. Effect of the structural configuration on the dynamic response

The influence of the longitudinal and transverse layout of the cable-system is addressed in this section (see Figures 9(a) and 9(b)).

Figure 9(a) presents the peak acceleration along the bridge centreline under the centered passing vehicle (Load Case I). This load case is selected to remove the contribution of torsional and local flange modes. It is observed

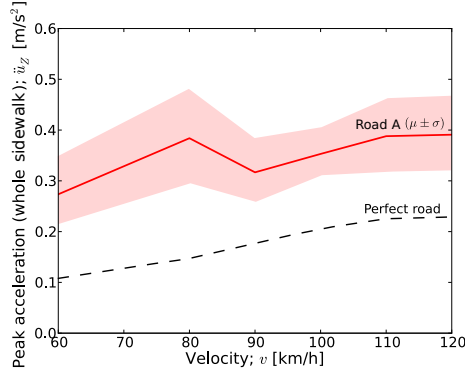


Figure 8: Influence of vehicle velocity ( $v$ ) on the peak vertical acceleration recorded in the whole sidewalk 1. Centered vehicle (Load Case I). BI-CONC-LEB bridge.

that the vertical acceleration along the longitudinal axis of the deck is reduced in the model with 15 distributed diverting struts in comparison with the models including only two struts at thirds of the total span, regardless of the transverse cable arrangement (concentrated or expanded). The largest reduction of the vertical vibration with the multiple-strut model (up to 25 %) is observed at quarters of the total span, where the configurations with two struts tend to concentrate the peak vertical acceleration due to the vibration of the side spans. This situation is avoided in the model with multiple (15) struts. The interaction between the cable-system and the deck seems more efficiently distributed in the model with multiple struts, and it results in reduced accelerations.

If the passing vehicle is centered (Load Case I) the dynamic response of the bridge is not influenced by the transverse cable arrangement because torsion is not activated. Only the eccentric vehicle (Load Case II and III) is able to differentiate the response with different transverse cable layouts, and the best way to look at this effect is to present the peak accelerations recorded across the deck width in Figure 9(b). In this figure it is observed that the vertical acceleration in sidewalk 1, close to the vehicle action, is 40-45 % lower in the model with struts concentrated in the mid-plane (BI-CONC-LEB) in contrast with solutions in which the struts are distributed across the deck width. Local flange modes are not exclusively responsible for this effect because the deck is the same in all the cases. Instead, it may be explained by high-order torsional modes of the deck coupled with the transverse movement of the struts. In the model with concentrated struts the triangular geometry

constrains the transverse movement of the point where the struts are joined. The frequency of this vibration mode in the model with concentrated struts (19.0 Hz) is higher than in the model with expanded struts (15.2 Hz), in which a stronger coupling with the vertical excitation of the flanges is also observed and contributes to the increment of acceleration in the sidewalks.

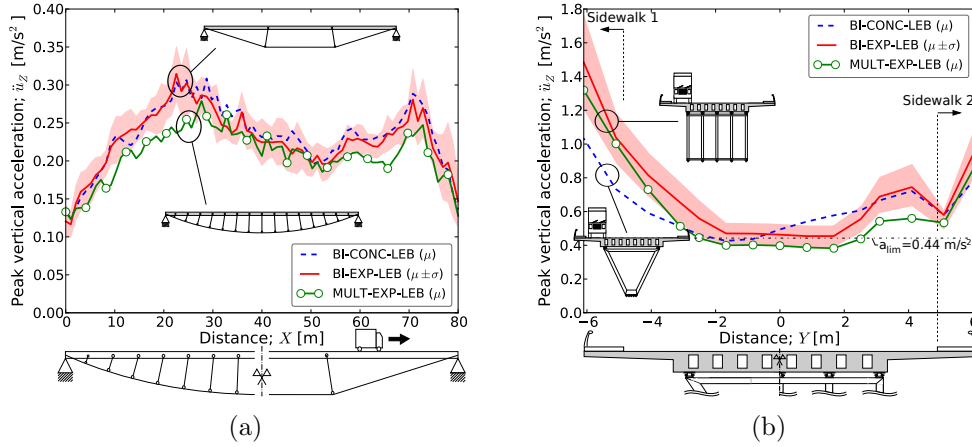


Figure 9: Influence of longitudinal and transverse cable arrangement; (a) peak vertical acceleration along the bridge centreline (Load Case I); (b) peak vertical acceleration in the whole bridge for different positions across the deck width (Load Case II). Road with very good pavement (road A) and maximum vehicle velocity:  $v = 120$  km/h.

In this work, the response of the bridge under traffic loading with different support conditions is also explored. From the comparison of the peak vertical acceleration along the deck in the model with two concentrated struts and very good road quality (road A), it is observed that the influence of support conditions is only appreciable close to the abutments, provided that both LEB and POT are very stiff in the vertical direction. This result was to be expected from the weak influence of support conditions on the first vertical vibration modes (see Table 2). It is verified that the peak vertical acceleration of the cantilevers near the supports is only slightly higher (by up to 10 %) when supports with a certain vertical flexibility (LEB) are replaced by infinitely stiff devices (POT).

## 6. Accuracy of simplified methodologies for assessing the SLS of vibrations

Finally, in this section, the SLS of vibrations is assessed by means of four different analysis methodologies with increasing accuracy and complexity: (i) equivalent static analysis; (ii) pseudo-static approach; (iii) dynamic analysis with Point Loads (PL); and (iv) dynamic analysis with Vehicle-Bridge Interaction (VBI) between a MDOF truck and the deck surface. The latter approach has been defined previously and the results obtained were discussed in previous sections. In the PL dynamic analysis the vehicle velocity is described by means of a set of nodal forces with a time-dependent amplitude defined in Figure 1(a). Taking advantage of the fact that the analysis is completely linear in the PL approach (no contacts are defined), the system of dynamics could be decoupled. For that reason, modal response history analysis is employed using frequencies up to 50 Hz.

The static and pseudo-static methods are deflection-based procedures that limit the maximum displacements under static loading to indirectly control the vibration. In the purely static procedure the action considered is the frequent live load defined as 50 % of the characteristic value in Eurocode EN1991-2:2003 [36]: 4.32 kN/m<sup>2</sup>, load uniformly distributed over the whole carriageway (Load Case I), or half the carriageway (Load Case II) in Figure 3(a); and two 600 kN point loads at mid-span with the eccentricity related to the studied Load Case (spaced 1.2 m apart). The maximum admissible deflection in the static approach is  $L/1000 = 8$  cm [12]. In the pseudo-static approach suggested by Smith [9], the peak acceleration is estimated by multiplying a dynamic load factor by the maximum static deflection ( $\delta_{c,\max}$ ) under the H20-44 truck action ( $Q$  loads in Figure 1(a)) located at mid-span, with the specific eccentricity. The maximum allowable acceleration in BS 5400 [19] is considered to obtain the following displacement limit,  $\delta_{\text{lim}}$ , (in m) in the pseudo-static approach:

$$\delta_{\max} \leq \left( \frac{2Lf - v}{8\pi^2 f^2 v} \right) \sqrt{f} = \delta_{\text{lim}} \quad (4)$$

where  $f$  is the first bridge frequency [Hz] and  $v$  is the vehicle velocity [m/s].

In order to facilitate the comparison of results, a safety factor is defined as the ratio between the admissible and the peak deflection or acceleration recorded in the structure:  $F_S = a_{\text{lim}}/a_{\text{max}}$ . Table 4 collects the safety factor in deflection-based criteria, whereas Table 5 includes the minimum safety

Table 4: Safety factor  $F_S$  associated with the SLS of vibrations for the deflection-based methodologies. If  $F_S < 1$  the SLS of vibrations is not satisfied.

Method	Velocity; $v$	Load Case	
		LC I	LCII
Static		1.00	1.08
Smith	60 km/h	12.90	9.44
	120 km/h	5.46	4.00

factor obtained employing acceleration-based dynamic procedures with different load cases and road qualities (for  $v = 120$  km/h). If  $F_S > 1$ , the SLS of vibrations is satisfied.

The shortcomings of the deflection-based approaches (both static and pseudo-static) are clearly observed by comparing Tables 4 and 5. Although the increment of vibration with the vehicle velocity is captured in the pseudo-static (Smith’s) procedure, the vibration problems caused by the H20-44 truck are significantly underpredicted in comparison with the dynamic methods that employ the same vehicle loading and the same BS 5400 criterion. The deflection-based methods inherently assume that the first vertical vibration mode governs the response. This assumption was proved to be erroneous earlier in this article. Furthermore the road quality and the vehicle users comfort are ignored in this type of analysis. In comparison with the most rigorous VBI dynamic approach, the deflection-based approaches presented in Table 4 could lead to a dramatic underestimation of the vibration perceived by pedestrians on the sidewalk if the road quality is not very good and/or the passing vehicles are eccentric. Both dynamic (acceleration-based) approaches adequately consider the position of the vehicle and the important dynamic contribution of torsional and local flange modes. However, the Point Load (PL) method ignores the vehicle dynamics and its interaction with the structure, which leads to peak accelerations in the sidewalks that are lower than those values obtained with the VBI model. The PL analysis method also prevents the study of the vehicle users comfort. In addition, the critical effect of the road roughness is only captured with the VBI approach because the irregularity profiles can be imposed at the contact points. VBI dynamic analyses are recommended in the design of slender bridges like UD-CSBs, specially if the road may deteriorate due to insufficient maintenance.

The influence of the road quality is definitively observed in Table 5. Only the roads with very good quality (A) satisfy the BS 5400 comfort crite-

Table 5: Safety factor  $F_S$  associated with the SLS of vibrations for the acceleration-based dynamic analysis methodologies with different comfort criteria, road qualities and Load Cases (LC). If  $F_S < 1$  the SLS of vibrations is not satisfied. VBI stands for Vehicle Bridge Interaction with MDOF truck model and PL for Point Load. The standard deviation is represented between brackets when pavement roughness is included. Vehicle velocity  $v = 120$  km/h. BI-CONC-LEB model.

Method	Road quality	Pedestrians (sidewalk 1)				Vehicle users	
		BS 5400-2		Irwin (frequent event)		LCI	LCII
		LC I	LCII	LCI	LCII		
PL	Perfect	2.6	1.5	0.9	0.8		
VBI	Perfect	1.9	0.6	0.7	0.3	6.5	5.6
	A	1.2(0.2)	0.4(0.1)	0.5(0.05)	0.2(0.03)	5.1(0.6)	3.3(0.5)
	B	0.7(0.1)	0.2(0.02)	0.3(0.05)	0.1(0.01)	3.5(0.4)	2.2(0.2)
	C	0.3(0.1)	0.2(0.04)	0.1(0.02)	0.08(0.01)	1.7(0.2)	1.1(0.1)
	D	0.2(0.03)	0.07(0.03)	0.08(0.01)	0.04(5E-3)	1.0(0.1)	0.7(0.1)

tion [19], whilst Irwin’s (considering the base curve for frequent events) [17] is not fulfilled in any case when  $v = 120$  km/h. If the road quality is not very good (B-D), the vibration that would be sensed by pedestrians is considered inadmissible regardless of the vehicle position. Highways are expected to fall in category A, but major roads may have B or even C pavement quality levels. The position of the vehicle with respect to the bridge axis is also very important in the SLS of vibrations. If the vehicle is eccentric (Load Case II) the maximum vertical acceleration recorded in the corresponding sidewalk exceeds the admissible BS 5400 limit even if the road quality is perfect (with the VBI analysis).

The safety factors obtained according to BS 5400 criterion are 2-3 times higher than those provided by Irwin when considering his base curve for everyday events, and 2-3 times lower than those resulting from the storm conditions. The discussion on the adequacy of both comfort criteria is beyond the scope of this work, but Irwin’s curve for storm conditions is not recommended by the authors since it would only cover infrequent events with more than one-year return period.

In order to address the comfort of the driver and passengers in the vehicle, the vertical acceleration of the truck cabin ( $\ddot{z}_u(t)$  in Figure 1(b)) is obtained from the time-history records of the vertical acceleration of the vehicle gravity centre ( $\ddot{z}_c(t)$ ) and its pitching acceleration ( $\ddot{\theta}_c(t)$ ), considering rigid body

motions. The vibration filtering from the seat is not considered herein. The dominant frequency of the vertical vibration sensed by vehicle users is obtained from the DFT analysis of the truck acceleration in the driver cabin ( $\ddot{z}_u(t)$ ). The DFT analyses conducted have enough resolution (0.1 Hz) to discriminate important peaks in the low-frequency range. In order to achieve this resolution, the length of the exiting platform is extended so that the total duration of the signal is 10 s regardless of the vehicle velocity (including the approach, forced vibration response, and free vibration phases). Figure 10 shows the DFT of the cabin acceleration for different vehicle velocities. It is observed that the dominant frequency is only shifted from 1.0 to 0.8 Hz by doubling the vehicle velocity from 60 to 120 km/h. From Figure 10 it is also clear that different energy peaks in the range between 0.8 and 1.6 Hz significantly contribute to the total vehicle response. However, the human comfort is barely sensitive to variations of the vibration frequency in this range. This may be inferred from the weighting factor defined by ISO 2631:1997-1 [11] to affect the r.m.s. value of  $\ddot{z}_u(t)$  and account for the higher admissible acceleration when seated: variations of the frequency between 0.8 and 1.6 Hz only increase the weighting factor from 0.477 to 0.494. A weighting factor of 0.48 is considered in this study. Although perception thresholds for whole-body vibration vary widely among individuals, the admissible acceleration of 1 m/s<sup>2</sup> (r.m.s.) is adopted to distinguish uncomfortable vibrations [11]. The ratio between this admissible acceleration and the weighted value (r.m.s.) recorded in VBI analyses is included in Table 5. It is observed that pedestrian's comfort is more critical than that of the vehicle users, verifying the Irwin's assumption [17]. The irregularity conditions of the road are also very important for the people inside the car. If the road quality is very good or good (A-B) the weighted vertical acceleration in the truck cabin is below 0.5 m/s<sup>2</sup> r.m.s., which lies between little and fairly uncomfortable in the scale of ISO 2631. However, if the road conditions are bad (D) the vibration could exceed the uncomfortable threshold (1 m/s<sup>2</sup>), especially if the vehicle is eccentric (Load Case II and III), due to the global torsional response of the bridge.

## 7. Conclusions

In this work, the response of innovative Under-Deck Cable-Stayed Bridges (UD-CSBs) under traffic loading is studied by means of rigorous finite element models and nonlinear dynamic analysis including a novel definition of

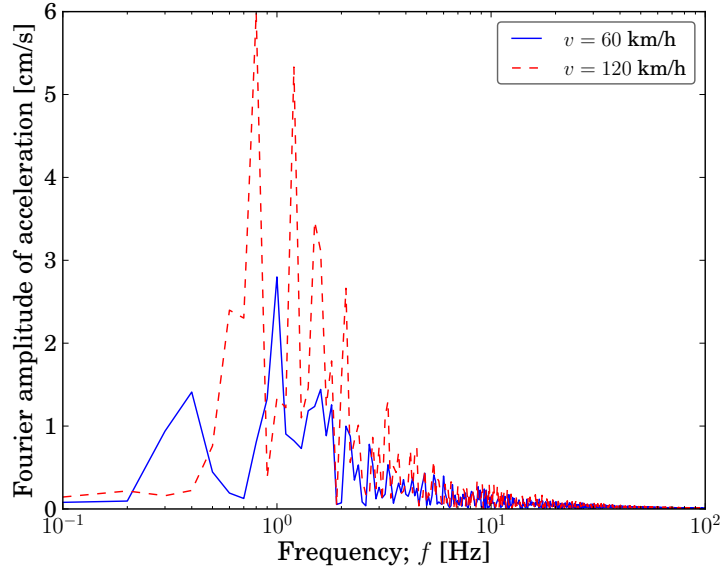


Figure 10: Frequency content of the vertical cabin acceleration for different velocities. Load Case I, perfect pavement. BI-CONC-LEB bridge.

the vehicle dynamics and its interaction with the structure. The following conclusions can be drawn.

An innovative Vehicle-Bridge Interaction model is proposed, taking into account the cross slope of the road and the finite dimensions of the truck wheels in the road profiles that are imposed at the contact points of the vehicle. The proposed disk model is recommended in light of the response obtained with different wheel radii, especially if the road quality is not very good and/or the wheel dimensions are large.

It was verified that design criteria based upon the assumption that the response is governed by the fundamental vertical flexural mode cannot hope to reflect the complex dynamic response of UD-CSBs. This is especially true if the passing vehicle is eccentric because in this case torsional modes and local flange modes with frequencies as high as 40 Hz have a significant contribution on the recorded acceleration along the sidewalks. These locations are particularly important due to the low tolerance of pedestrians to experience vertical vibration. Three-dimensional finite element models are recommended in vibration serviceability analyses of these structures, paying attention to adequately capture the global torsion and the local vertical

flexure in the flanges.

The definition of the weight, speed, and dynamic properties of the heavy vehicles to be considered for the assessment of the serviceability limit state of vibration is essential. However, these parameters are not considered in most of the design codes related to loading for road bridges. Further research in this area is recommended in order to be able to perform accurate and realistic analysis for this limit state in slender road bridges.

The number of struts deviating the cable-system in UD-CSBs moderately effects the peak acceleration recorded. If multiple (15) struts are employed, the vibration is reduced at quarters of the total span in comparison with models including only two diverting struts. The influence of the cable arrangement in the transverse direction is stronger, but it is only clear if the passing vehicle is eccentric with respect to the bridge central axis. The solution with concentrated cables in the mid-plane reduces the peak vertical acceleration on the sidewalk (by up to 45 %). The type of bearings deployed does not play a significant role in effecting the response, provided that they are well designed.

The SLS of vibrations has been checked with different analysis procedures and comfort criteria. Considering the results obtained with the most precise method (Vehicle-Bridge Interaction) and according to BS 5400-2, the vibration would be only admissible by pedestrians if the road quality is very good (A). That is, the maintenance of the road is paramount for satisfying the SLS of vibrations. The comfort of vehicle users is less critical than that of pedestrians in all the cases. Nevertheless, it has been observed that people inside the car could perceive uncomfortable vibrations when crossing the bridge if the road quality is poor (D) and the vehicle is not in the central road lane.

From the point of view of the analysis strategy, the deflection-based approaches (static and pseudo-static) are discouraged since they rely on the false assumption that the structure is controlled by the fundamental mode. On the other hand, the simplified dynamic analysis with moving point loads could be used for preliminary analysis but may be unconservative because the road quality is ignored. The Vehicle Bridge Interaction method is recommended for the detailed design of UD-CSBs.

## References

- [1] Ruiz-Teran, AM, Aparicio, AC. Verification criteria of the sls of vibrations for road bridges with slender prestressed concrete decks. *in*: International FIB Symposium, London (UK); 2009.
- [2] Ruiz-Teran, AM, Aparicio, AC. Two new types of bridges: under-deck cable-stayed bridges and combined cable-stayed bridges - the state of the art. *Can J Civ Eng* 2007; 34: 1003–1015.
- [3] Ruiz-Teran, AM, Aparicio, AC. Parameters governing the response of under-deck cable-stayed bridges. *Can J Civ Eng* 2007; 34: 1016–1024.
- [4] Ruiz-Teran, AM, Aparicio, AC. Structural behaviour and design criteria of under-deck cable-stayed bridges and combined cable-stayed bridges. Part I: single-span bridges. *Can J Civ Eng* 2008; 35: 938–950.
- [5] Ruiz-Teran, AM, Aparicio, AC. Structural behaviour and design criteria of under-deck cable-stayed bridges and combined cable-stayed bridges. Part II: multispan bridges. *Can J Civ Eng* 2008; 35: 951–962.
- [6] Ruiz-Teran, AM, Aparicio, AC. Response of under-deck cable-stayed bridges to the accidental breakage of stay cables. *Eng Struct* 2009; 26: 1425–1434.
- [7] Camara, A, Ruiz-Teran, AM, Stafford, PJ. Structural behaviour and design criteria of under-deck cable-stayed bridges subjected to seismic action. *Earthq Eng Struct Dyn* 2013; 42: 891–912.
- [8] Ruiz-Teran, AM, Aparicio, AC. Unconventional cable-stayed bridges. structural behaviour and design criteria. *Structural Concrete* 2010; 11: 25–34.
- [9] Smith, J, *Vibration of structures, applications in civil engineering design*. Chapman and Hall, 1988.
- [10] Demic, M, Lukic, J, Milic, Z. Some aspects of the investigation of random vibration influence on ride comfort. *J Sound Vib* 2002; 253: 109–129.
- [11] ISO 2631:1997: Mechanical vibration and shock – Evaluation of human exposure to whole-body vibration Part 1: General requirements. 1997.

- [12] American Association of State Highway and Transportation Officials. AASHTO LRFD: Bridge design specifications. 2nd Edition Washington, 1998.
- [13] Roeder, C, Barth, K, Bergman, A. Effect of live-load deflections on steel bridge performance. *J Bridge Eng* 2004; 9; 259–267.
- [14] Recommendations for the project of composite road bridges, RPX-95 (*in Spanish*). Madrid, 2003.
- [15] Shahabadi, A. Bridge Vibration Studies. Joint Highway Research Project. Technical Report, Purdue University & Indiana State Highway Commission, Rep. No. JHRP 77-17, 1977.
- [16] Heinemeyer, C, Butz, C, Keil, A, Schlaich, M, Goldack, A, Trometer, S, Lukic, M, Chabrolin, B, Lemaire, A, Martin, PO, Cunha, A, Caetano, E. Design of lightweight footbridges for human induced vibrations, JRC Scientific and Technical Reports, EUR 23984 EN, 2009.
- [17] Irwin, A. Human response to dynamic motion of structures. *The Structural Engineer* 1978; 56A: 237–244.
- [18] Zivanovic, S, Pavic, A, Reynolds, P. Vibration serviceability of footbridges under human-induced excitation: a literature review. *J Sound Vib* 2005; 279: 1–74.
- [19] British Standard BS 5400-2. Steel, concrete and composite bridges - Part-2: Specification for loads, 2006.
- [20] Griffin, MJ. Discomfort from feeling vehicle vibration. *Vehicle System Dynamics* 2007; 45; 7-8; 679–698.
- [21] Marchesiello, S, Fasana, A, Garibaldi, L, Piombo, B. Dynamics of multi-span continuous straight bridges subject to multi-degrees of freedom moving vehicle excitation. *J Sound Vib* 1999; 224; 541–561.
- [22] Deng, L, Cai, C. Development of dynamic impact factor for performance evaluation of existing multi-girder concrete bridges. *Eng Struct* 2010; 32; 21–31.
- [23] Zhu, X, Law, S. Dynamic load on continuous multi-lane bridge deck from moving vehicles. *J Sound Vib* 2002; 251; 697–716.

- [24] European Committee for Standardization. EN 1337-3:2005 Structural bearings. Part 3: Elastomeric bearings, 2005.
- [25] Ramberger, G. Structural Bearings and Expansion Joints for Bridges (IABSE), volume 6, ISBN: 3-85748-105-6, Switzerland, 2002.
- [26] ABAQUS. User's manual version 6.12., 2012.
- [27] Schlaich, M, Werwigk, M. The Glacis bridge in Ingolstadt, Germany, *in: IABSE symposium, Seoul, 2001.*
- [28] Nakagawa, T, Okada, T, Hamazaki, Y, Okada, N, Mochiduki, H, Nagai, M. Structural characteristics of a cable-trussed bridge. *in: IABSE symposium, Seoul, 2001.*
- [29] Yang, Y, Lin, C. Vehicle-bridge interaction dynamics and potential applications. *J Sound Vib 2005: 284; 205–226.*
- [30] ISO 8608:1995: Mechanical vibration - Road surface profiles - Reporting of measured data, International Standard ISO, Geneva. 1995.
- [31] Coussy, O, Said, M, Van Hoove, J. The influence of random surface irregularities on the dynamic response of bridges under moving loads. *J Sound Vib 1989: 130; 313–320.*
- [32] Kamash, K, Robson, J. The application of isotropy in road surface modelling. *J Sound Vib 1978: 57; 89–100.*
- [33] Captain, K, Boghani, A, Wormley, D. Analytical tire models for dynamic vehicle simulation. *Vehicle Syst Dyn 1979: 8; 1–32.*
- [34] Chang, K, Wu, F, Yang, Y. Disk model for wheels moving over highway bridges with rough surfaces. *J Sound Vib 2011: 330; 4930–4944.*
- [35] Moghimi, H, Ronagh, H. Development of a numerical model for bridge-vehicle interaction and human response to traffic-induced vibration. *Eng Struct 2008: 30; 3808–3819.*
- [36] European Committee for Standardization. EN 1991-2:2003: Traffic loads on bridges, 2003.